ACS OMEGA

http://pubs.acs.org/journal/acsodf

Article

Simultaneous Cross-type Detection of Water Quality Indexes via a Smartphone-App Integrated Microfluidic Paper-Based Platform

Xiaolu Xiong, Chengwang Guo, Gengyang Yan, Bingxin Han, Zan Wu, Yueqian Chen, Shiqi Xu, Peng Shao, Hong Song,* Xiyan Xu,* and Junfeng Han*

Cite This: *ACS Omega* 2022, 7, 44338−44345

Read Online

ACCESS | Metrics & More | Article Recommendations | Supporting Information

ABSTRACT: Water quality guarantee in remote areas necessitates the development of portable, sensitive, fast, cost-effective, and easy-to-use water quality detection methods. The current work reports on a microfluidic paper-based analytical device (μPAD) integrated with a smartphone app for the simultaneous detection of cross-type water quality parameters including pH, Cu(II), Ni(II), Fe(III), and nitrite. The shapes, baking time, amount, and ratios of reaction reagent mixtures of wax μPAD were optimized to improve the color uniformity and intensity effectively. An easy-to-use smartphone app was established for recording, analyzing, and directly reading the colorimetric signals and target concentrations on μPAD. The results showed that under the optimum conditions, the current analytical platform has reached the detection limits of 0.4, 1.9, 2.9, and 1.1 ppm for nitrite, Cu(II), Ni(II), and Fe(III), respectively, and the liner ranges are 2.3−90 ppm (nitrite), 3.8−400 ppm (Cu(II)), 2.9−1000 ppm (Ni(II)), 2.8−500 ppm (Fe(III)), and 5−9 (pH). The proposed portable smartphone-app integrated μPAD detection system was successfully applied to real industrial wastewater and river water quality monitoring. The proposed method has great potential for field water quality detection.

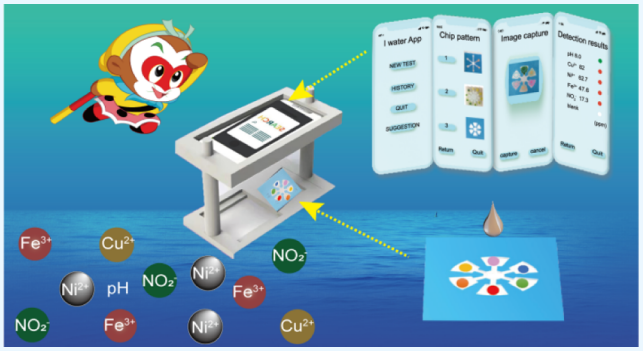

1. INTRODUCTION

The industrial expansion inevitably produces a variety of pollution sources, deteriorating the quality of natural water bodies and seriously threatening the ecosystem and human health, which speed up the requirement for efficient novel detection methods for water quality monitoring.[1−3] This is even more necessary for the water quality guarantee in remote and uninhabited water areas, where expensive and heavy water quality detecting equipment cannot be conveniently used. Therefore, it is essential to develop portable, sensitive, fast, cost-effective, and easy-to-use water quality detection methods.

Among the harmful pollutants in water, nitrite (NO_2^-) can lead to diseases such as methemoglobinemia or stomach cancer through the formation of carcinogenic *N*-nitrosamines.[4,5] The accumulation of toxic heavy metal ions Cu(II), Ni(II), and Fe(III) increases the risk of anemia, cancers,[6] neurological, immune disorders, and so forth.[7,8] Simultaneously, contamination of these anions and cations may cause the pH value to exceed the usual safety range 6.5−9.5[9] and result in abnormal heart rhythm, neuromuscular irritability, and even coma.[10] To date, a lot of analytical methods have been reported for monitoring water quality, such as capillary electrophoresis, inductively coupled plasma atomic emission spectrometry,[11] ion chromatography,[12] and high-performance liquid chromatography.[13] However, those techniques not only rely on expensive instruments and highly skilled technicians but also require a long detection time.

Microfluidic paper-based analytical devices (μPADs) have been widely used as promising alternatives for water pollutant detection.[14−16] Integration of colorimetric detection on μPADs allows the analysis of multiple water quality indexes through color signals from specific chromogenic reactions.[17−19] For example, Fang Li et al. constructed a three-dimensional microfluidic paper-based device to determine six metal ions-Fe(III), Ni(II), Cr(VI), Cu(II), Al(III), and Zn(II).[20] Kamnoet et al. developed a device with two pretreatment zones for simultaneous determination of Cu(II), Co(II), Ni(II), Hg(II), and Mn(II).[11] However, those works could only detect metal ions which are not capable for cross-type water quality index monitoring. Our previous work used a UV exposure method to fabricate a μPAD for simultaneous detection of two types of analytes, including heavy metal ions Fe(III), Ni(II), and BSA.[21] Janegitz group used μPAD for monitoring Ca(II), Mg(II), total

Received: September 13, 2022
Accepted: November 9, 2022
Published: November 23, 2022

Scheme 1. Schematic of the Fabrication and Application of the Smartphone-App Integrated μPAD System

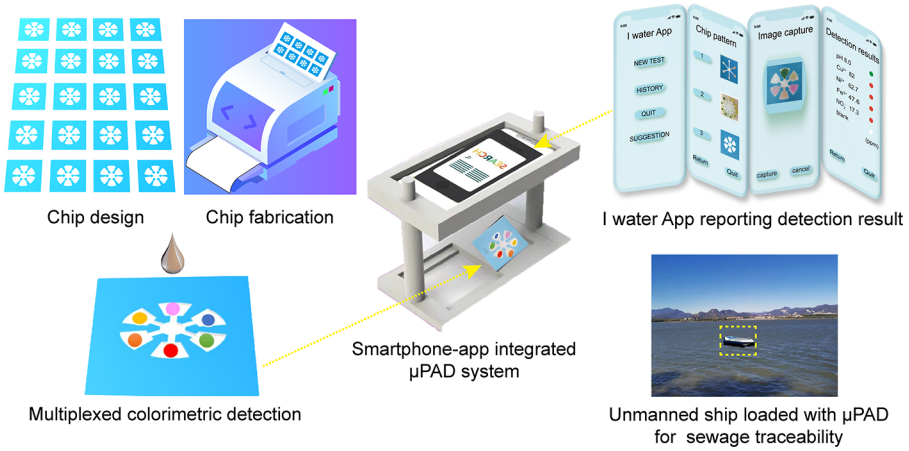

phenols, and pH.[10] These works increased the types of analytes on one analytical platforms. However, it still has many drawbacks, for example, it takes time and effort of users to identify and judge the detection results.

Integration of smartphones and sensors is a promising way to achieve fast, portable, and easy-to-use detection of water pollutants.[22−25] However, in some applications, the smartphone only plays the role of collecting the colorimetric signal, lacking data storage and analysis function.[26−29] The further integration of μPAD with a smartphone app provides an excellent strategy for smart on-site analysis.[30−33] Zheng et al. developed a μPAD integrated with a smartphone app for simple and portable analysis of glucose and uric acid.[31] While the smartphone app platform has brought great convenience to field detection,[30] the multifunctional features of a smartphone app have not been fully exploited.

In this work, we developed a smartphone-app integrated μPAD detection system for simultaneous and fast (5 min) detection of cross-type multiple water quality parameters including pH, Cu(II), Ni(II), Fe(III), and nitrite. For that purpose, (1) the pattern of the flower-shaped μPAD, (2) the baking time and temperature of the wax chip, (3) the reagent volume for the chip, and (4) the proportion of the reaction mixture solution were optimized. Using the optimized conditions, color palettes for each analyte were obtained (Scheme 1). By extracting the chromaticity value of each color, the standard curves between color intensity and logarithmic concentration were established. Then, an "I-water" smartphone app was developed to store the standard curves and "read" the chroma yielded after a new reaction. An external support system was constructed to ensure the proper connection between μPADs and smartphones, which "translate" the chip result into concentration information for the users. The proposed system has great potential in field water quality detection on an unmanned ship (Scheme 1). The aim of this work is to provide a portable, sensitive, fast, and cost-effective water quality detection system.

2. MATERIALS AND METHODS

2.1. Chemicals and Instruments. Sodium nitrite, nickel-(II) sulfate hexahydrate, and the standard solutions (Cu(II), Fe(III), Na(I), Co(II), Mg(II), Ca(II), Cd(II), and Al(III)) were purchased from Sigma-Aldrich Corp. Bathocuproine, dimethylglyoxime (DMG), hydroxylammonium chloride, ammonium acetate, sodium fluoride (NaF), sodium citrate, ammonium hydroxide, hydrochloric acid, polyethylene glycol (PEG) 600, paraaminobenzenesulfonic acid, *N*-(α-naphthyl)-ethylenediamine dihydrochloride (NED), citric acid, phenanthroline, BTB, disodium hydrogen phosphate solution, and sodium dihydrogen phosphate solution were purchased from Aladdin Industrial Corp. All reagents used in the experiment were of analytical grade and used without purification. 2 mg/mL DMG solution was prepared individually with ethanol. 1 g/mL hydroxylammonium chloride solution, 0.156 g/mL ammonium acetate solution, 0.5 M NaF, and 10 mM sodium citrate buffer solution were diluted with ultrapure water. 1.9−400 ppm Cu(II), 2.9−1000 ppm Ni(II), 1.1−500 ppm Fe(III), and 0.4−90 ppm nitrite were prepared by dissolving mother liquor in ultrapure water. The samples of standard pH values were prepared with sodium dihydrogen phosphate hydrochloric acid, disodium hydrogen phosphate, and ammonia ranging from 5 to 9.

Whatman grade 1 filter paper (Whatman International Ltd, UK) was chosen as the hydrophilic material. Wax printer (Xerox ColorQube8580, UK) and hot plate (kaisi 818, China) were used to form hydrophobic area. The pH was measured by a pH meter (Lichen PH-10, China). Inductively coupled plasma mass spectrometry (ICP−MS, spectro MS, China) provided a standard method for validation.

2.2. Fabrication of μPADs and the Support System. The pattern was designed in Adobe illustrator software. Each pattern includes 4 × 5 μPADs, and each μPAD (40 × 40 mm) consists of a center zone (6 mm diameter) and six detection zones connected by microchannels (2 mm width, 2.8 mm long). The pattern was printed on a Whatman 1 filter paper by a wax ink printer and heated on the hot plate to completely melt the wax, forming a stable hydrophobic barrier. Then, the patterned paper was cut into 20 μPADs for detection.

A two-layered bracket was established for fixing a smartphone and a μPAD. The lower layer is used to load μPAD and the upper layer for smartphone. The distance between the smartphone and the μPAD is adjustable.

2.3. Colorimetric Detection of Cu(II), Ni(II), Fe(III), Nitrite, and pH. For Cu(II) detection, bathocuproine was used as the colorimetric reagent that reacted with Cu(II), forming an orange complex. Hydroxylamine hydrochloride was added to the detection zones for reducing Cu(II) to Cu(I). Acetic acid/NaCl buffer (pH 4.5) was used to set the pH at the detection reservoir and Cl^- to stabilize the orange $Cu(Bc)_2$ products. The dried PEG was pipetted to reduce the hydrophobicity in the

https://doi.org/10.1021/acsomega.2c05938
ACS Omega 2022, 7, 44338−44345

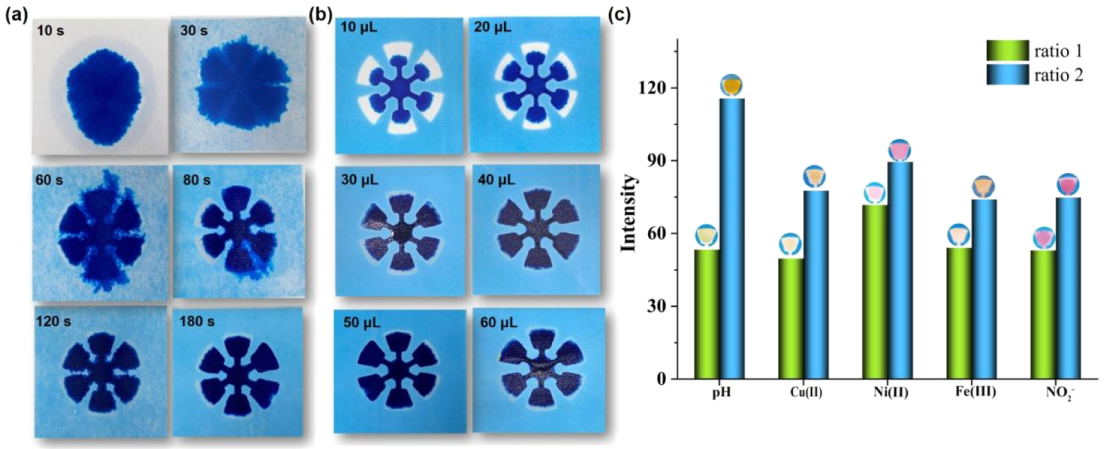

Figure 1. Parameter optimization for μPAD fabrication. (a) Baking time: 10, 30, 60, 80, 120, and 180 s. (b) Solution amounts: 10, 20, 30, 40, 50, and 60 μL. (c) Reaction solution ratio optimization for detection of pH (1 and 10%), Cu(II) 1:1:2:1 (ratio 1) and 1:1:4:2 (ratio 2), Ni(II) 2:1:4:1 (ratio 1) and 2:1:5:2.5 (ratio 2), Fe(III) 1:1:1 (ratio 1) and 1:2:1 (ratio 2), and NO_2^- 1:1:1 (ratio 1) and 1:1:3 (ratio 2). Inset: Corresponding images of the paper chips after reactions.

detection reservoir caused by bathocuproine. The analysis of Ni(II) was achieved by using DMG as a sensitive colorimetric reagent to produce a pink complex. NaF works as the masking reagent to avoid the interference of Fe(III) and Co(II). The optimum value of pH 9.0 was adjusted by ammonium hydroxide for the chromogenic reaction. Hydroxylamine hydrochloride worked as a mask for Cu(II), Zn(II), and Co(II). Fe(III) was reduced into Fe(II) by hydroxylammonium chloride. 1,10-Phenanthroline was used to react with Fe(II) to form an orange complex. Ammonium acetate provided the acidic environment for the chromogenic reaction. For the detection of nitrite, the Griess reagent (330 mM citric acid, 50 mM paraaminobenzenesulfonic acid, and 10 mM NED solution) reacted with nitrite, causing a pink color. For the detection of pH, BTB was prepared as a hydrogen potential indicator. With the increase in pH, BTB changes from the protonated indicator structure to a deprotonated form. Thus, the yellow color in the detection zone becomes darker until it turns blue.

2.4. Simultaneous Colorimetric Detection and Image Analysis. First, the reagent solution for Cu(II), Fe(III), Ni(II), pH, and nitrite were added on detection zones of μPAD, standard solutions for five analytes were injected into the central zone. Then the color response occurred in each detection zone between the analytes and the corresponding indicator. The images of color palettes were taken by a smartphone, and the color intensity was measured by ImageJ software. Then, calibration curves were established by drawing the functional relationship between the color intensity and the concentration of each analyte.

2.5. Smartphone App for Cross-type Real Water Quality Index Detection. An "I water" smartphone app was developed for contaminant detection on android platform, including four steps:

[1] Obtaining information. The nonlinear RGB pixel information of the color signal on the μPAD captured by the smartphone was extracted and calculated through formula 1.

$$R' = R/255, \quad G' = G/255, \quad B' = B/255,$$
$$C\ \max = \max(R', G', B'), \quad C\ \min = \min(R', G', B'),$$
$$\Delta = C\ \max - C\ \min \tag{1}$$

[2] Image preprocessing. Denoising and smoothing operations were done to remove the redundant image information and highlight the image features.

[3] Extracting and selecting image features. The nonlinear RGB pixels of the color signal in the image was linearized according to the mathematical relationship from formula 2. The corresponding HSV value distribution was obtained to realize feature extraction.

$$H = \begin{cases} 0^\circ & \Delta = 0 \\ 60^\circ \times \left(\dfrac{G' - B'}{\Delta} + 0\right), & C\ \max = R' \\ 60^\circ \times \left(\dfrac{B' - R'}{\Delta} + 2\right), & C\ \max = G' \\ 60^\circ \times \left(\dfrac{R' - G'}{\Delta} + 4\right), & C\ \max = B' \end{cases}$$

$$S = \begin{cases} 0 & C\ \max = 0 \\ \Delta / C\ \max & C\ \max \neq 0 \end{cases}$$

$$V = C\ \max \tag{2}$$

[4] Design of the classifier and classification strategy. The target to be detected was classified, and the concentration characteristics through the fitting curve were calculated to realize the analysis of the image.

[5] Real water sample analysis. The data of color palettes and calibration curves stored in the "I water" app can be used as references for actual sample analysis. After adding the real water sample to the center zone of μPAD, the "I water" smartphone app started running for on-site real water sample analysis.

3. RESULTS AND DISCUSSION

3.1. μPAD Optimization. Appropriate shape and size of μPADs patterns are critical for the flow of reaction solution and the homogeneity of colorimetric reaction in multiple analytical applications. Several types of μPADs patterns were designed and tested, including tree-shaped (Figure S1a) and multichannel types (Figure S1b–d). Among them, the flower-shaped pattern

https://doi.org/10.1021/acsomega.2c05938
ACS Omega 2022, 7, 44338−44345

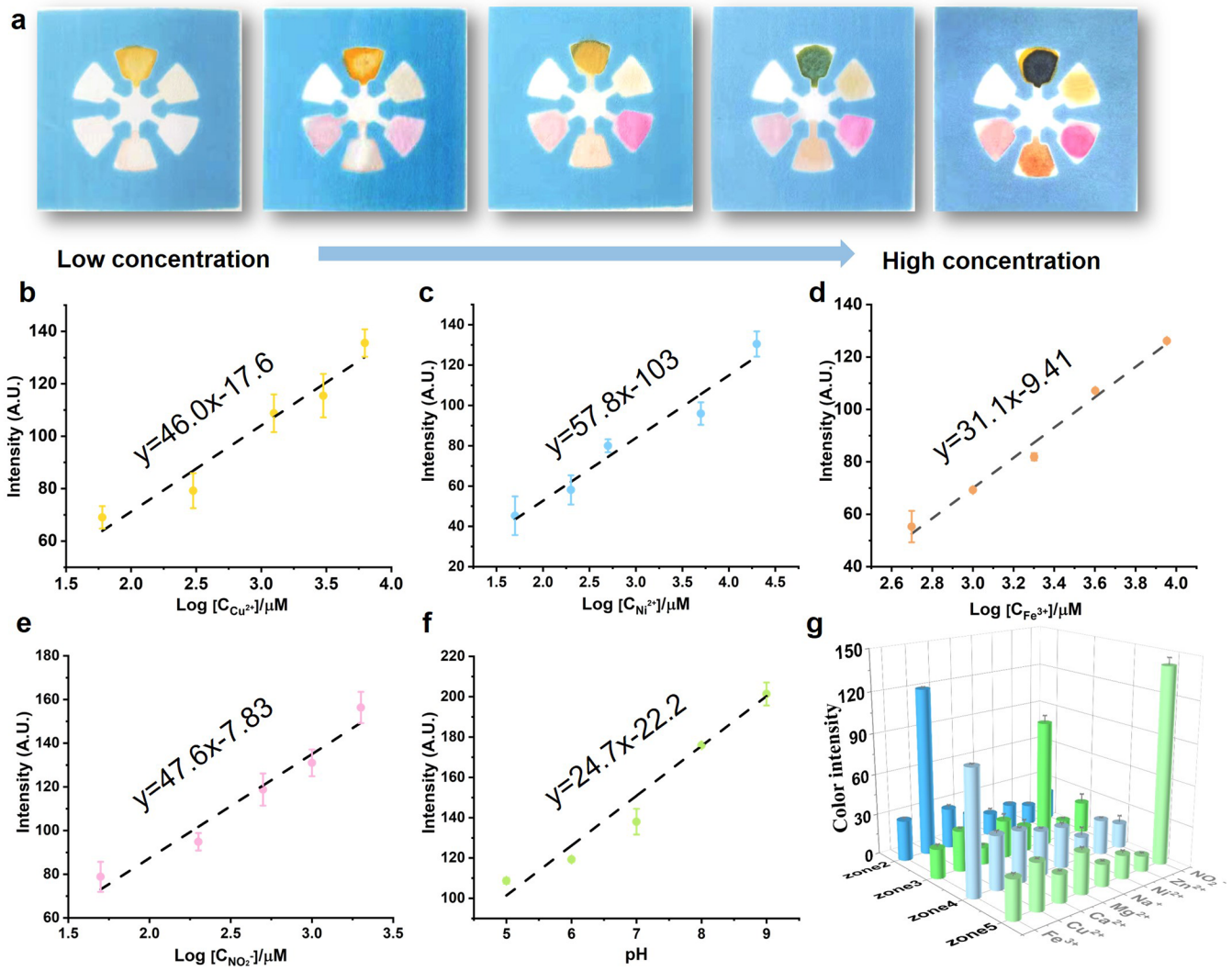

Figure 2. Color palettes for visual simultaneous determination of Cu(II) (yellow), Ni(II) (magenta), Fe(III) (orange), nitrite (rosy), and pH (dark yellow to blue). The concentration for each palette is as follows: Cu(II), Ni(II), Fe(III), and nitrite with concentration of 1.9, 5.9, 2.8, and 1.4 ppm (palette 1); 19.2, 58.7, 56, and9.2 ppm (palette 2); 38.4, 293.5, 112, and 23 ppm (palette 3); 192, 587, 280, and 46 ppm (palette 4); and 400, 990, 448, and 90 ppm (palette 5). In addition, pH was 5, 6, 7, 8, and 9 for each palette. Calibration curves between color intensity and log target concentration for (b) Cu(II), (c) Ni(II), (d) Fe(III), (e) NO_2^-, and (f) pH. The error bars represent standard deviation (SD) obtained from three independent measurements (n = 3). (g) Interference study of the μPAD. Color intensities were obtained from the detection zone 2−5 (Cu(II), Ni(II), Fe(III), NO_2^-, reaction reagents added) in the presence of NO_2^-, Zn^{2+}, Ni^{2+}, Na^+, Mg^{2+}, Ca^{2+}, Cu^{2+}, and Fe^{3+}.

with a short channel and a fan ring-shaped detection zone (Scheme 1d) can achieve homogeneity of the solution flow in the channel and uniformity of color presentation on the detection areas. Therefore, this structure is adopted in the following study.

The baking temperature and time are key factors in forming a high-quality hydrophobic area for wax-printing μPAD. The baking temperatures were optimized to be 150 °C (Figure S2). The baking time was optimized by injecting methylene blue solution into the flow passage of μPAD to indicate the hydrophilic zone. Figure 1a shows the back views of the μPAD after injecting methylene blue solution into the flow passage. Baking time less than 120 s provided an incomplete hydrophobic area on the back of the chip because the wax ink does not completely penetrate into the whole paper. For the baking time of 180 s, the indicator solution was dispersed within the pattern area, and the hydrophobic areas were completely formed on the back of the paper. Therefore, 180 s was chosen as the best baking time in the following experiment. This heating step is part of fabricating the μPAD in the lab. When we use the prepared μPAD for on-spot detection, the heating step is not involved.

To achieve the best performance of the μPAD, the impact of the amount of solution added in the μPAD channel was checked using methylene blue solution (10−60 μL) as the indicator. As shown in Figure 1b, 10 to 40 μL of solution was insufficient to fill up the detection zones. However, volumes greater than 60 μL caused the solution to spread out the flow channel. Therefore, the optimal reagent volume is set at 50 μL in the subsequent experiments.

It is also important to optimize the ratio of chromogenic reagent, buffer, and masking agents for a clear and multiple presentation of the color reaction on the μPAD. For pH detection, BTB and alcohol at 1% and 10% ratios were tested. The ratio of 10% (ratio 2) allowed a contrast among different pH values and showed 116.8% increase in color intensity (Figure 1c,

https://doi.org/10.1021/acsomega.2c05938
ACS Omega 2022, 7, 44338−44345

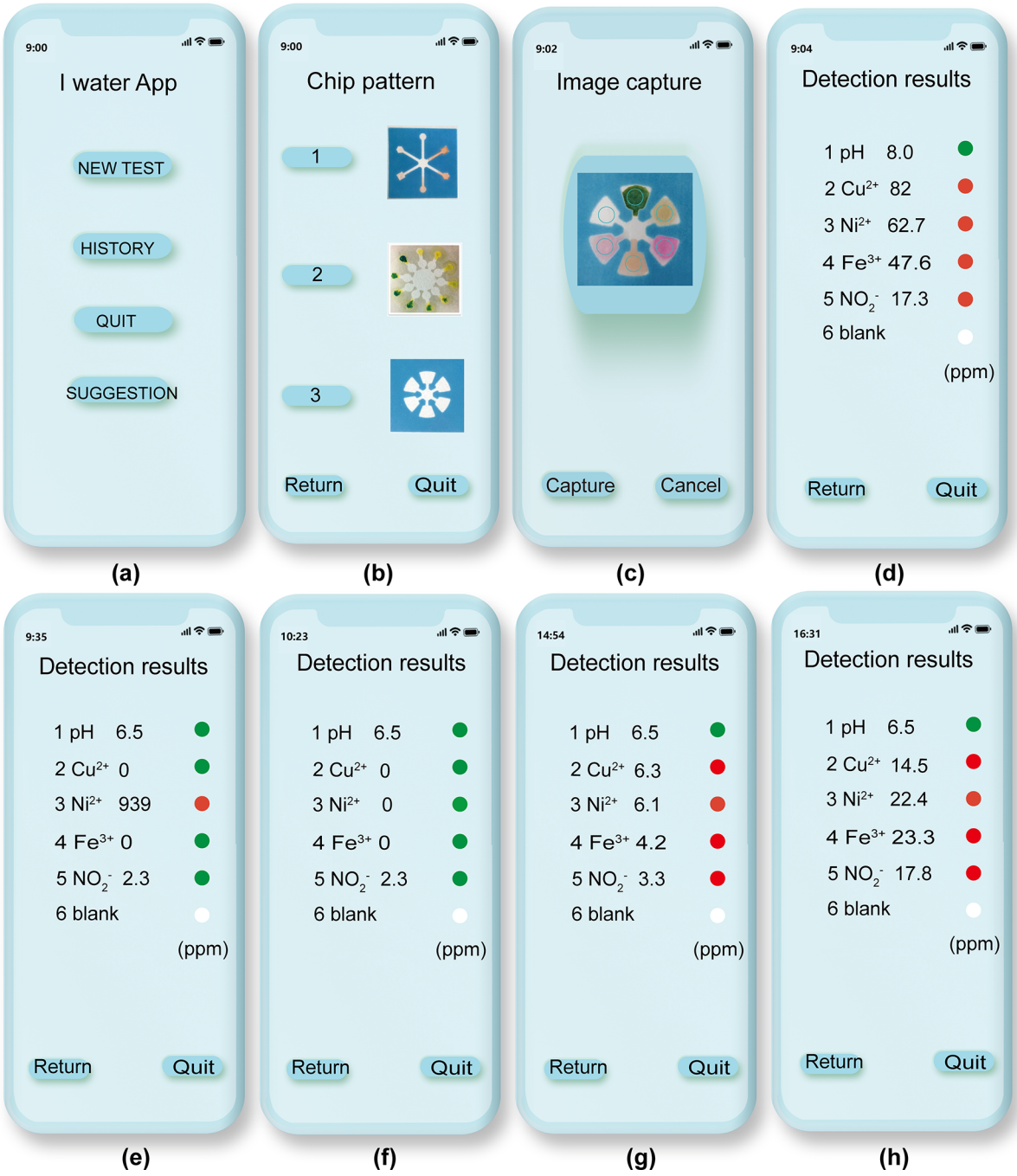

Figure 3. Images for each functional interface of the "I water" smartphone-app. (a) Main menu interface, (b) Chip pattern selection interface, (c) Image capture interface, and (d) Detection result interface. The red dot represents the ion content exceeding the standard, the green dot represents the ion concentration fit for the standard, and the white dot represents the blank control. Results of smartphone app for determination of Cu(II), Ni(II), Fe(III), NO_2^-, and pH in (e) raw industrial water, (f) purified industrial water sample, and (g,h) spiked river water samples 1 and 2.

pH). For Cu(II) detection, hydroxylamine hydrochloride, ammonium acetate, bathocuproine acetone solution, and PEG600 are mixed in the proportion of 1:1:2:1 (ratio 1) and 1:1:4:2 (ratio 2) as the reaction mixture solution. For 60 ppm Cu(II) detection, the color intensity enhanced more than 56.3% by increasing the bathocuproine acetone ratio from 1:1:2:1 to 1:1:4:2 [Figure 1c, Cu(II)]. Furthermore, the color intensity turned saturated with a further increase of the bathocuproine acetone. Thus, 1:1:4:2 was chosen as the optimum ratio. Similarly, for Ni(II) detection, as the ratio of sodium fluoride, acetic acid, DMG, and ammonium hydroxide solution increased from 2:1:4:1 to 2:1:5:2.5, the intensity increased by 24.7% for detecting 58 ppm Ni(II). Thus the ratio of 2:1:5:2.5 was considered as the optimum condition for further study [Figure 1c, Ni(II)]. For the colorimetric reaction of Fe(III), ammonium acetate, 1,10-phenanthroline, and hydroxylammonium chloride solution at 1:1:1 (ratio 1), 1:2:1 (ratio 2) were mixed and tested. The color intensity improved by more than 36.7% and reached the peak at the ratio of 1:2:1 [Figure 1c, Fe(III)]. For the colorimetric reaction of NO_2^-, 330 mM citric acid, 50 mM paraaminobenzenesulfonic acid, and 10 mM NED solution were mixed at 1:1:1 (ratio 1) and 1:1:3 (ratio 2), and the intensity

https://doi.org/10.1021/acsomega.2c05938
ACS Omega 2022, 7, 44338−44345

reached its maximum value at the ratio of 1:1:3 (Figure 1c, NO_2^-).

3.2. Performance of the μPADs. Simultaneous cross-type detection of multiple water quality indexes was carried out and is shown in Figure 2a. The position of the alarm clock at 12 o'clock is the detection zone #1, and the color plate is clockwise from detection zones #1 to 6. Among them, detection zones #1−5 on the μPAD were modified for pH, Cu(II), Ni(II), Fe(III), and NO_2^-, respectively, and the detection zone #6 was blank for comparison. It can be observed that the blue (or dark yellow) pH complexes, orange $Cu(Bc)_2$, pink $Ni(DMG)_2$, rosy NO-$(NED)^{2-}$, and orange $Fe(phen)_3^{2-}$were produced in detection zones #1 to 5. The color gets darker accordingly with the increases of concentration for each analyte.

Quantitative detection of Cu(II), Ni(II), Fe(III), nitrite, and pH can be realized by establishing calibration curves between the color intensity and logarithmic concentration of each analyte in a wide range. A linear relationship was established between color intensity and logarithmic concentration of Cu(II) with the linear range of 3.8−400 ppm (R^2 = 0.978) (Figure 2b) and a detection limit of 1.9 ppm. The detection limit for Ni(II) was 2.9 ppm within 2.9−1000 ppm (R^2 = 0.960) (Figure 2c). The linear range for Fe(III) was 2.8−500 ppm (Figure 2d) with the lowest detectable concentration of 1.1 ppm (R^2 = 0.986). For nitrite, the linear range was 2.3−90 ppm (Figure 2e) with a detection limit of 0.4 ppm (R^2 = 0.960). Regarding pH, the linear range was pH 5−9 (Figure 2f). In general, the detection limit of the current μPAD for Cu(II), Ni(II), Fe(III), nitrite, and pH is close to the regulation requirement for water.[9]

To evaluate the effects of other ions on the detection of the target ions Cu(II), Ni(II), Fe(III), or NO_2^-, the interference of three of them on the rest one was checked (pH interference on zone #1 was not considered due to quite different reaction reagents from metal ions). At the same time, the interference of Ca(II), Mg(II), Na(I), and Zn(II) were also considered since they are typical interferences in drinking water and polluted water body.[11] As shown in Figure 2g, the observed color intensity from detection zone #2 is high in the presence of Cu(II), but are much smaller in the presence of other interfering ions. Similarly, the color intensity from Ni(II), Fe(III), NO_2^- detection zone #3−5 are high in the presence of Ni(II), Fe(III), and NO_2^-, respectively, but are much smaller in the presence of other analytes. This phenomenon occurred because the specific colorimetric reaction were achieved by involving Cu(II), Ni(II), Fe(III), and NO_2^-, demonstrating a high selectivity of the current μPAD toward Cu(II), Ni(II), Fe(III), and NO_2^-.

3.3. Smartphone-App Integrated μPAD for the Real Water Quality Detection. We expanded the μPAD detection to other analytes, such as Co(II) and Mn(II) (Figure S3). The abovementioned results on the performance of the μPAD for multiple water quality parameter detection set a solid basis for the following smartphone application. The "I water" smartphone app was designed for the fast detection of water quality indexes, and the operational scheme is shown in Figure 3, including (a) I-water app starting, (b) chip pattern selection, (c) image capture, and (d) detection results report steps. Compared with the other self-developed apps for image processing, the developed "I-water" app has obvious novelty in the aspects of sewage over standard judgment, multiple pattern choice, and detection result tracking.

First, the "I-water" app has an added over standard alarm function. The national standard specifies the content of each water analyte. Once the detection concentration exceeds the standard content, a red color spot is immediately observed on the interface of the app. In that way, it is very convenient for user to judge whether the water content is not healthy. Besides, the I-water app has a special interface for selecting different chip patterns. Lists of chip patterns were designed and fabricated according to different detection environments, such as industrial wastewater, agricultural water, or a water source. Each user can select the corresponding chip pattern based on the actual detection requirements. In addition, the "History" function can compare the detection results of the latest period. In that way, we can conveniently track water quality changes. In summary, the powerful app is expected as convenient tool for field water analysis.

The availability of the smartphone-app integrated μPAD detection system was evaluated by detecting real industrial wastewater and natural river water samples. The industrial wastewater was obtained from an electronic factory in Suzhou, Jiangsu Province, China. For the raw industrial wastewater sample of the electronic factory (Figure 3e), the test results of the smartphone app were 939 ppm Ni(II), 2.3 ppm NO_2^-, pH 6.5, and Cu(II), Fe(III) were not detected, demonstrating that the Ni(II) content of this electronic factory effluent exceeded the waste water discharge requirement. The World Health Organization guideline value for nitrite and Ni(II) is 3 and 0.5 ppm.[9] After the wastewater was treated by the sewage treatment plant, the smartphone integrated μPAD system was further used to test the purified wastewater, as shown in Figure 3f, pH value was 6.5, 2.3 ppm NO_2^-, with no detectable Cu(II), Ni(II), and Fe(III). Comparing the results of the two tests, it can be concluded that our detection method can monitor industrial wastewater discharge and effectively supervise wastewater treatment.

The river water was first sampled in Zunyi, Guizhou Province. The results of smartphone-app integrated μPAD detection system demonstrate that the river is not polluted by Cu(II), Ni(II), Fe(III), and NO_2^- (Figure S4a). Further, 6.4 ppm Cu(II), 5.8 ppm Ni(II), 3.9 ppm Fe(III), and 3.9 ppm NO_2^- were spiked to the river samples, respectively. According to the app result (Figure 3g), 6.3 ppm Cu(II), 6.1 ppm Ni(II), 4.2 ppm Fe(III), and 3.3 ppm nitrite were detected, and the pH value was 6.5. The relative SD (RSD) of the smartphone-app result and the added amounts is less than 5% (Table 1). In addition, the river sample 2 obtained from the Beijing physical and chemical analysis and testing center also reached a similar conclusion (Figure S4b). When 14.8 ppm Cu(II), 22.8 ppm Ni(II), 22.4 ppm Fe(III), and 18.4 ppm NO_2^- were added to the river sample 2, smartphone app reported that 14.5 ppm Cu(II), 22.4 ppm Ni(II), 23.3 ppm Fe(III), 17.8 ppm nitrite, and pH 6.5

Table 1. Comparison of pH, NO_2^-, Cu(II), Ni(II), and Fe(III) Detection Using the Smartphone-App Integrated μPAD and the ICP−MS Method

sample	target	added (ppm)	found (ppm)	ICP−MS (ppm)	RSD (%)	recovery (%)
sample 1	Cu(II)	6.4	6.3	6.2	3.12	98.4
	Ni(II)	5.8	6.1	6.0	4.34	105.1
	Fe(III)	3.9	4.2	4.1	2.65	107.6
	NO_2^-	3.1	3.3	3.2	3.05	106.4
sample 2	Cu(II)	14.8	14.5	14.6	4.35	97.9
	Ni(II)	22.8	22.4	23.1	3.23	98.2
	Fe(III)	22.4	23.3	23.1	1.38	104.0
	NO_2^-	18.4	17.8	17.9	3.12	96.7

https://doi.org/10.1021/acsomega.2c05938
ACS Omega 2022, 7, 44338−44345

(Figure 3h) were detected. Thus, the developed smartphone-app integrated μPAD system can work well if the river has been polluted by heavy metal ions or NO_2^-.

3.4. Accuracy and Reliability of the Smartphone-App Integrated μPAD System. The accuracy and reliability of smartphone-app integrated μPAD detection system were investigated by comparing with detection results of ICP−MS. As shown in Table 1, the test results of the smartphone-app integrated μPAD showed no significant difference with those of the standard ICP−MS method, validating the accuracy of the smartphone-app integrated μPAD system. Then, the reliability of the system was further investigated by recovery experiments. The recoveries and RSD % ranges were calculated to be 97.9−98.4% and 3.12−4.35% for Cu(II), 98.2−105.1% and 3.23−4.34% for Ni(II), 104.0−107.6% and 1.38−2.65% for Fe(III), 96.7−106.4% and 3.05−3.12% for nitrite, respectively. Thus, the reliability of the smartphone-app integrated μPAD system is acceptable.

It is worth mentioning that the analysis time (within 5 min) for the μPAD-combined smartphone-app method is much shorter than that of ICP−MS. The combination of the cost-effective portable μPAD and a smartphone app as the signal readout makes the water quality detection method user-friendly and efficient, which shows great potential for on-site real water analysis.

4. CONCLUSIONS

A smartphone-app integrated μPAD was developed for highly efficient detection of cross-type multiple water quality indexes including NO_2^-, Cu(II), Ni(II), Fe(III), and pH. The optimal conditions were determined to achieve the detection limit of 0.4, 1.9, 2.9, and 1.1 ppm for NO_2^-, Cu(II), Ni(II), Fe(III), and 5 for pH, respectively. Interference study showed the high anti-interference ability of this system. It successfully achieved the fast detection (within 5 min) of the water quality indexes of real industrial wastewater and river water samples. The comparison of the detection performance of the current smartphone-app integrated μPAD method and ICP−MS further confirmed its accuracy and efficiency. It should be noted that more water quality indices, other than the five tested in the current study, can be easily detected when more kinds of chromogenic reagents are used, indicating the promising potential application of the current method for on-site real water analysis on an unmanned ship.

■ ASSOCIATED CONTENT

Supporting Information

The Supporting Information is available free of charge at https://pubs.acs.org/doi/10.1021/acsomega.2c05938.

Several types of μPAD patterns, baking temperature optimization for fabricating μPADs, calibration curves for detection of Co(II) and Mn(II), and smartphone-app results for determination of river water samples 1 and 2 (PDF)

■ AUTHOR INFORMATION

Corresponding Authors

Hong Song − *School of Computer Science and Technology, Beijing Institute of Technology, Beijing 100081, China*; Email: anniesun@bit.edu.cn

Xiyan Xu − *School of Chemistry and Chemical Engineering, Beijing Institute of Technology, Beijing 102488, China*; Email: xiyanxu@bit.edu.cn

Junfeng Han − *Centre for Quantum Physics, Key Laboratory of Advanced Optoelectronic Quantum Architecture and Measurement (MOE), School of Physics, Beijing Institute of Technology, Beijing 100081, China; Yangtze Delta Region Academy of Beijing Institute of Technology, Jiaxing 314000, China*; orcid.org/0000-0002-8671-966X; Email: pkuhjf@bit.edu.cn

Authors

Xiaolu Xiong − *Centre for Quantum Physics, Key Laboratory of Advanced Optoelectronic Quantum Architecture and Measurement (MOE), School of Physics, Beijing Institute of Technology, Beijing 100081, China; Yangtze Delta Region Academy of Beijing Institute of Technology, Jiaxing 314000, China*; orcid.org/0000-0001-8441-6027

Chengwang Guo − *Centre for Quantum Physics, Key Laboratory of Advanced Optoelectronic Quantum Architecture and Measurement (MOE), School of Physics, Beijing Institute of Technology, Beijing 100081, China*

Gengyang Yan − *School of Computer Science and Technology, Beijing Institute of Technology, Beijing 100081, China*

Bingxin Han − *Centre for Quantum Physics, Key Laboratory of Advanced Optoelectronic Quantum Architecture and Measurement (MOE), School of Physics, Beijing Institute of Technology, Beijing 100081, China*

Zan Wu − *Institute of Analysis and Testing, Beijing Academy of Science and Technology, Beijing Center for Physical and Chemical Analysis, Beijing 100089, China*

Yueqian Chen − *Centre for Quantum Physics, Key Laboratory of Advanced Optoelectronic Quantum Architecture and Measurement (MOE), School of Physics, Beijing Institute of Technology, Beijing 100081, China*

Shiqi Xu − *Centre for Quantum Physics, Key Laboratory of Advanced Optoelectronic Quantum Architecture and Measurement (MOE), School of Physics, Beijing Institute of Technology, Beijing 100081, China; Yangtze Delta Region Academy of Beijing Institute of Technology, Jiaxing 314000, China*

Peng Shao − *Institute of Analysis and Testing, Beijing Academy of Science and Technology, Beijing Center for Physical and Chemical Analysis, Beijing 100089, China*

Complete contact information is available at: https://pubs.acs.org/10.1021/acsomega.2c05938

Notes

The authors declare no competing financial interest.

■ ACKNOWLEDGMENTS

This work was funded by the National Natural Science Foundation of China (NSFC) (11734003 and 62275016), the National Key Research and Development Program of China (2020YFA0308800 and 2021YFC2102205), and the Beijing Natural Science Foundation (no. Z210006).

■ REFERENCES

(1) Attaallah, R.; Amine, A. Highly selective and sensitive detection of cadmium ions by horseradish peroxidase enzyme inhibition using a colorimetric microplate reader and smartphone paper-based analytical device. *Microchem. J.* **2022**, *172*, 106940.

(2) Noviana, E.; Ozer, T.; Carrell, C. S.; Link, J. S.; McMahon, C.; Jang, I.; Henry, C. S. Microfluidic Paper-Based Analytical Devices: From Design to Applications. *Chem. Rev.* **2021**, *121*, 11835−11885.
(3) Xu, X.; Liu, Y.; Liu, S.; Li, J.; Guo, G.; Smith, K. Real-time detection of potable-reclaimed water pipe cross-connection events by conventional water quality sensors using machine learning methods. *J. Environ. Manage.* **2019**, *238*, 201−209.
(4) Hou, C.-Y.; Fu, L.-M.; Ju, W.-J.; Wu, P.-Y. Microfluidic colorimetric system for nitrite detection in foods. *Chem. Eng. J.* **2020**, *398*, 125573.
(5) Yu, P.; Deng, M.; Yang, Y.; Nie, B.; Zhao, S. 3D microfluidic devices in a single piece of paper for the simultaneous determination of nitrite and thiocyanate. *Sensors* **2020**, *20*, 4118.
(6) Ninwong, B.; Ratnarathorn, N.; Henry, C. S.; Mace, C. R.; Dungchai, W. Dual sample preconcentration for simultaneous quantification of metal Ions using electrochemical and colorimetric Assays. *ACS Sens.* **2020**, *5*, 3999−4008.
(7) Sivakumar, R.; Lee, N. Y. Recent progress in smartphone-based techniques for food safety and the detection of heavy metal ions in environmental water. *Chemosphere* **2021**, *275*, 130096.
(8) Sun, X.; Li, B.; Qi, A.; Tian, C.; Han, J.; Shi, Y.; Lin, B.; Chen, L. Improved assessment of accuracy and performance using a rotational paper-based device for multiplexed detection of heavy metals. *Talanta* **2018**, *178*, 426−431.
(9) World Health Organization. *A Global Overview of National Regulations and Standards for Drinking-Water Quality*, 2018. 978-92-4-151376-0.
(10) da Silva, V. A. O. P.; de Freitas, R. C.; de Oliveira, P. R.; Moreira, R. C.; Marcolino-Junior, L. H.; Bergamini, M. F.; Coltro, W. K. T.; Janegitz, B. C. Microfluidic paper-based device integrated with smartphone for point-of-use colorimetric monitoring of water quality index. *Measurement* **2020**, *164*, 108085.
(11) Kamnoet, P.; Aeungmaitrepirom, W.; Menger, R. F.; Henry, C. S. Highly selective simultaneous determination of Cu(II), Co(II), Ni(II), Hg(II), and Mn(II) in water samples using microfluidic paper-based analytical devices. *Analyst* **2021**, *146*, 2229−2239.
(12) Feng, S.; Caire, R.; Cortazar, B.; Turan, M.; Wong, A.; Ozcan, A. Immunochromatographic diagnostic test analysis using Google Glass. *ACS Nano* **2014**, *8*, 3069−3079.
(13) Aksorn, J.; Teepoo, S. Development of the simultaneous colorimetric enzymatic detection of sucrose, fructose and glucose using a microfluidic paper-based analytical device. *Talanta* **2020**, *207*, 120302.
(14) Qin, X.; Liu, J.; Zhang, Z.; Li, J.; Yuan, L.; Zhang, Z.; Chen, L. Microfluidic paper-based chips in rapid detection: current status, challenges, and perspectives. *TrAC, Trends Anal. Chem.* **2021**, *143*, 116371.
(15) Yakoh, A.; Chaiyo, S.; Siangproh, W.; Chailapakul, O. 3D capillary-driven paper-based sequential microfluidic device for electrochemical sensing applications. *ACS Sens.* **2019**, *4*, 1211−1221.
(16) Qi, Q.; Li, B.; Wang, X.; Fu, L.; Luo, L.; Chen, L. Rotational paper-based microfluidic-chip device for multiplexed and simultaneous fluorescence detection of phenolic pollutants based on a molecular-Imprinting technique. *Anal. Chem.* **2018**, *90*, 11827−11834.
(17) Jang, I.; Carrão, D. B.; Menger, R. F.; Moraes de Oliveira, A. R. M. D.; Henry, C. S. Pump-free microfluidic rapid mixer combined with a paper-based channel. *ACS Sens.* **2020**, *5*, 2230−2238.
(18) Yin, K.; Ding, X.; Xu, Z.; Li, Z.; Wang, X.; Zhao, H.; Otis, C.; Li, B.; Liu, C. Multiplexed colorimetric detection of SARS-CoV-2 and other pathogens in wastewater on a 3D printed integrated microfluidic chip. *Sens. Actuators, B* **2021**, *344*, 130242.
(19) Jalal, U. M.; Jin, G. J.; Shim, J. S. Paper-plastic hybrid microfluidic device for smartphone-based colorimetric analysis of Urine. *Anal. Chem.* **2017**, *89*, 13160−13166.
(20) Li, F.; Hu, Y. T.; Li, Z. M.; Liu, J. C.; Guo, L.; He, J. B. Three-dimensional microfluidic paper-based device for multiplexed colorimetric detection of six metal ions combined with use of a smartphone. *Anal. Bioanal. Chem.* **2019**, *411*, 6497−6508.
(21) Xiong, X. L.; Zhang, J. L.; Wang, Z.; Liu, C. C.; Xiao, W. D.; Han, J. F.; Shi, Q. F. Simultaneous multiplexed detection of protein and metal ions by a colorimetric microfluidic paper-based analytical device. *Biochip* **2020**, *14*, 429−437.
(22) Lopez-Ruiz, N.; Curto, V. F.; Erenas, M. M.; Benito-Lopez, F.; Diamond, D.; Palma, A. J.; Capitan-Vallvey, L. F. Smartphone-based simultaneous pH and nitrite colorimetric determination for paper microfluidic devices. *Anal. Chem.* **2014**, *86*, 9554−9562.
(23) Xia, Y.; Chen, Y.; Tang, Y.; Cheng, G.; Yu, X.; He, H.; Cao, G.; Lu, H.; Liu, Z.; Zheng, S.-Y. Smartphone-based point-of-care microfluidic platform fabricated with a ZnO nanorod template for colorimetric virus detection. *ACS Sens.* **2019**, *4*, 3298−3307.
(24) Guo, X.-L.; Chen, Y.; Jiang, H.-L.; Qiu, X.-B.; Yu, D.-L. Smartphone-based microfluidic colorimetric sensor for gaseous formaldehyde determination with high sensitivity and selectivity. *Sensors* **2018**, *18*, 3141.
(25) Xu, D.; Huang, X.; Guo, J.; Ma, X. Automatic smartphone-based microfluidic biosensor system at the point of care. *Biosens. Bioelectron.* **2018**, *110*, 78−88.
(26) Kim, S. C.; Jalal, U. M.; Im, S. B.; Ko, S.; Shim, J. S. A smartphone-based optical platform for colorimetric analysis of microfluidic device. *Sens. Actuators, B* **2017**, *239*, 52−59.
(27) Hou, T.; Chang, H.; Jiang, H.; Wang, P.; Li, N.; Song, Y.; Li, D. Smartphone based microfluidic lab-on-chip device for real-time detection, counting and sizing of living algae. *Measurement* **2022**, *187*, 110304.
(28) Wood, C. S.; Thomas, M. R.; Budd, J.; Mashamba-Thompson, T. P.; Herbst, K.; Pillay, D.; Peeling, R. W.; Johnson, A. M.; McKendry, R. A.; Stevens, M. M. Taking connected mobile-health diagnostics of infectious diseases to the field. *Nature* **2019**, *566*, 467−474.
(29) Jiang, H.; Sun, B.; Jin, Y.; Feng, J.; Zhu, H.; Wang, L.; Zhang, S.; Yang, Z. A disposable multiplexed chip for the simultaneous quantification of key parameters in water quality monitoring. *ACS Sens.* **2020**, *5*, 3013−3018.
(30) Jiang, Q.; Wu, J.; Yao, K.; Yin, Y.; Gong, M. M.; Yang, C.; Lin, F. Paper-based microfluidic device (DON-Chip) for rapid and low-Cost Deoxynivalenol quantification in food, feed, and feed Ingredients. *ACS Sens.* **2019**, *4*, 3072−3079.
(31) Zheng, J.; Zhu, M.; Kong, J.; Li, Z.; Jiang, J.; Xi, Y.; Li, F. Microfluidic paper-based analytical device by using Pt nanoparticles as highly active peroxidase mimic for simultaneous detection of glucose and uric acid with use of a smartphone. *Talanta* **2022**, *237*, 122954.
(32) Sun, B. R.; Zhou, A. G.; Li, X.; Yu, H. Z. Development and application of mobile Apps for molecular sensing: A Review. *ACS Sens.* **2021**, *6*, 1731−1744.
(33) Liang, C.; Liu, Y.; Niu, A.; Liu, C.; Li, J.; Ning, D. Smartphone-app based point-of-care testing for myocardial infarction biomarker cTnI using an autonomous capillary microfluidic chip with self-aligned on-chip focusing (SOF) lenses. *Lab Chip* **2019**, *19*, 1797−1807.

https://doi.org/10.1021/acsomega.2c05938
ACS Omega 2022, 7, 44338−44345